

1 **The dynamical role of upper layer salinity in the Mediterranean Sea**

2 Ali Aydogdu¹, Pietro Miraglio¹, Romain Escudier², Emanuela Clementi¹, Simona Masina¹

3 ¹ Ocean Modeling and Data Assimilation Division, Fondazione Centro Euro-Mediterraneo sui Cambiamenti Climatici,
4 Bologna, Italy

5 ² Observations pour Les Systèmes D'analyse et de Prévision, Mercator Ocean International, Toulouse, France

6 *Correspondence to:* Ali Aydogdu (ali.aydogdu@cmcc.it)

7 **Abstract.**

8 The Mediterranean Sea is a semi-enclosed basin with an excess amount of evaporation compared to the water in-flux through
9 precipitation at the surface and river runoff on the land boundaries. The deficit in the water budget is balanced by the inflow
10 in the Gibraltar Strait and Turkish Straits System connecting the Mediterranean with the less saline Atlantic Ocean and the
11 Black Sea, respectively. There is evidence that the Mediterranean region is a hotspot in a warming climate which will possibly
12 change the water cycle significantly, but with large uncertainties. Therefore, it is inevitable to monitor the evolution of the
13 essential ocean variables to respond to the associated risks and mitigate the related problems. In this work, we evaluate the
14 evolution of the salinity content and anomaly between 0-300 m in the Mediterranean Sea during the last decades using the
15 Copernicus Marine Service reanalysis and in-situ objective analysis products. The results show an increasing mean salinity
16 with a stronger trend in the eastern basin. The spread of the products implies a larger variability in the western basin while
17 the standard deviation is lower in the eastern side, especially in the Ionian and the Levantine basins.

18

19 **Short summary.**

20 This paper investigates the salinity content and anomaly evolution in the Mediterranean Sea using observational and
21 reanalysis products. The salinity content increases overall while negative salinity anomalies appear in the western basin
22 especially around the upwelling regions. There is a large spread in the salinity estimates that reduces with the emergence of
23 the Argo era.

24 **1 Introduction**

25 The Mediterranean Sea is warming (Pisano et al., 2020). It is evaporating more and more (Skiriris et al., 2018; Jordà et al.,
26 2017) with marine heat waves increasing in intensity, duration and frequency (Juza et al., 2022; Dayan et al., 2022). The
27 Mediterranean region is a hotspot with global warming (Tuel and El Tahir, 2020) that will likely alter the water cycle (Cos
28 et al., 2022). Tracking the changes of the essential ocean variables (EOVs) is crucial in order to understand the impact of

29 climate change. Two of these EOVs are linked to the ocean salinity at the surface and subsurface, which will be affected
30 significantly by the surface heat and freshwater fluxes. The global water cycle modulating the ocean salinity is a key element
31 of the Earth's climate (Cheng et al., 2020). In the Mediterranean Sea, freshwater fluxes through the land (rivers) and
32 atmosphere (evaporation and precipitation) are balanced by two sea straits, namely Gibraltar and Dardanelles, from which
33 the less saline Atlantic Ocean and Black Sea waters flow into the basin with an annual net inflow of 0.78 ± 0.05 Sv (Soto-
34 Navarro et al., 2010) and 0.05 ± 0.04 Sv (Jarosz et al., 2013), respectively. These density contrasts contribute to the wind
35 driven circulation and generate a highly energetic anti-estuarine circulation (Cessi et al., 2014). The salinity of the Atlantic
36 water entering through the Gibraltar Strait is about 36.2 psu. The salinity of the Dardanelles can vary significantly and it can
37 be as low as 27 psu (Aydogdu et al., 2018; Sannino et al., 2017). Recently, Fedele et al. (2022) studied the characterization
38 of the Atlantic Waters (AW) and Levantine intermediate waters (LIW) from the ARGO profiles in the last 20 years. Their
39 conclusion is a clear salinification and warming trend which characterised both AW and LIW over the last two decades.
40 Skliris et al. (2018) argue that the Mediterranean basin salinification is driven by changes in the regional water cycle rather
41 than by changes in salt transports at the straits, as it is shown by the water mass transformation distribution in salinity
42 coordinates. However, we will show that there is a bigger uncertainty compared to most of the basin in the radius of influence
43 of both the Gibraltar and Dardanelles Straits. In Section 2, the data and methods used in this study are presented. In Section
44 3, the results are shown and discussed, while in Section 4 the conclusions are drawn.

45 **2 Data and method**

46 In this study, Copernicus Marine Service global and regional reanalysis as well as observational gridded products are used to
47 explore the role of the salinity variability in the 0-300 m depth among different estimates as well as temporal and spatial
48 anomalies against a mean.

49 The Mediterranean $1/24^\circ$ resolution regional reanalysis (hereinafter, MEDREA24; Escudier et al., 2021) from Copernicus
50 Marine Service is used as a regional high-resolution product. In this work, MEDREA24 and its interim extension until the
51 end of 2021 are included. Moreover, the $1/4^\circ$ resolution Global Reanalysis Ensemble Product (hereinafter, GREP) is also
52 used. It consists of the global reanalysis from Mercator Ocean's GLORYS2V4 (Lellouche et al., 2013), UK MetOffice's
53 GLOSEA5v13 (MacLachlan et al., 2014) using the FOAM system (Blockley et al., 2014), CMCC C-GLORSv7 (Storto et
54 al., 2016) and ECMWF's ORAS5 (Zuo et al., 2017). A study on the ocean heat content and steric sea level representation in
55 the GREP ensemble can be found in Storto et al. (2019a). A more general status of the global ocean reanalysis is reviewed
56 in Storto et al. (2019b). The period covered by the GREP is 1993-2019.

57 As observational products, the CORA (Szekely et al., 2019) and ARMOR3D (Guinehut et al., 2012) gridded reconstructions
58 are adopted. Both datasets are available between 1993 and 2020. In the CORA, the objective analysis is performed on
59 measurement's anomalies relative to a first guess provided by World Ocean Atlas 2013 monthly climatology for different

60 decades, to accurately reproduce the climate tendencies, is interpolated and centred on the 15th of each month. Instead in
 61 ARMOR3D, the first guess is adopted from World Ocean Atlas 2018. Both products use an objective analysis method
 62 proposed by Bretherton et al., (1976).

63 The investigation is performed in the entire Mediterranean Sea as well as in the eastern and western basins, which have very
 64 different characteristics. The salinity mean (\bar{S}) is computed using formula (1) as the monthly volume (V) average of each
 65 product between 0 and 300 m depth, i.e., excluding the shelf areas close to the coast with a depth less than 300 m.

$$67 \quad \bar{S} = \frac{1}{V} \int_V S dV$$

66 (1)

68 The mean of different products and their standard deviation are evaluated in the common period 1993-2019. Besides this
 69 time frame, the CORA and ARMOR3D time series are available until 2020, while the MEDREA24 time series is provided
 70 up to 2021 (last 6 months extended in interim mode).

71 The salinity anomalies are computed using formula (2). The difference of the salinity, S , with a reference salinity, S_{ref} , is
 72 normalised by the depth of the water column which is constant in our case with $z_2 = 300$ m and $z_1 = 0$ m.

$$74 \quad S_A = \int_{z_1}^{z_2} \frac{S - S_{ref}}{z_2 - z_1} dz$$

73 (2)

75 Formula (2) is a modified version of the one proposed in Boyer et al. (2007) which uses the salinity as a proxy for the
 76 equivalent freshwater content. This method has been later adopted in various studies including, among the others, Holliday
 77 et al. (2020), with a density weight to account for baroclinic properties of the water column. The formulation in Boyer et al.
 78 (2007) is based on a reference salinity. As an example, mean values of a basin (Aagaard and Carmack, 1989) is a widely used
 79 choice for S_{ref} in global freshwater content calculations. However, it is argued that since a reference value can be chosen
 80 arbitrarily, this would bring ambiguity (Schauer and Losch, 2019) in computing the equivalent freshwater content. Therefore,
 81 in this study we propose to evaluate the salinity content and anomaly following formula (2) by choosing S_{ref} as a monthly
 82 climatology of each dataset computed from each product separately between 1993 and 2014. This period is chosen to be
 83 consistent with the Ocean Monitoring Indicators produced previously in the Mediterranean Sea and other Copernicus Marine
 84 domains. Furthermore, the calculations are performed in the entire Mediterranean Sea (MED) as well as in its western
 85 (WMED) and eastern (EMED) sub basins, separated at the Sicily Strait. In Fig. 1, we present the monthly variation of the
 86 S_{ref} , as an example only the one from MEDREA24, which shows a clear difference in the seasonality in the EMED and
 87 WMED, with a maximum in March and December, respectively. It is also evident that the Mediterranean monthly salinity

88 reference shows a seasonal cycle much similar to the one of the Eastern basin (but with different magnitude) characterised
89 by lower salinity during the summer period and larger values at the end of the year.

90 **3 Results and Discussion**

91 The Copernicus Marine service products described in the previous section allow the assessment of the salinity content of the
92 Mediterranean Sea along with its anomaly and trend during the last decades.

93 In Fig. 2, we present the time series of the mean salinity content in the first 300 m derived from the analysed products
94 (MEDREA24 in red; GREP ensemble mean in blue; GREP ensemble members in thin light blue; CORA in dark green,
95 ARMOR3D in light green) and their overall mean (in black) and spread (shaded grey).

96 In the early 90s in the entire Mediterranean Sea (Fig. 2a), there is a large spread in salinity with the observations showing a
97 higher salinity while the reanalysis products present relatively lower salinity. This is the case until 2005. Coinciding with the
98 global coverage of the Argo profilers in the early 2000s following the efforts in the Global Ocean Data Assimilation
99 (GODAE) together with the Climate Variability and Predictability Programme (CLIVAR) and the Global Climate Observing
100 System/Global Ocean Observing System (GCOS/GOOS), the spread among different products narrows. Possibly, the
101 reanalyses are better constrained through data assimilation with this novel observation type (Johnson et al., 2022) which
102 provides high-resolution and high-frequency temperature and salinity profiles all over the world' ocean while the observation-
103 based gridded products become more confident. The maximum spread between the period 1993-2019 is in the 90's with a
104 value of 0.096 psu and it decreases to as low as 0.009 psu by the end of 2010s. The mean salinity computed in the entire
105 Mediterranean Sea from all products varies between approximately 38.5 and 38.6 psu with a spatiotemporal mean of 38.57
106 psu (Table 1).

107 In the western Mediterranean (Fig. 2b), the overall mean is centred around 38.16 psu with a larger spread - with a maximum
108 and minimum of 0.172 psu and 0.026, respectively - occurring in the early 2000s. An increase of the mean salinity in 2005
109 is evident from all the reanalysis products and, at a lesser extent, from the CORA dataset, for which one of the many possible
110 reasons is the regime shift as discussed in (Schroeder et al., 2016) corresponding to a major deep water formation event at
111 the beginning of the Western Mediterranean Transition (Zunino et al., 2012).

112 In the eastern Mediterranean (Fig. 2c), the overall mean is centred around 38.87 psu with a lower spread compared to the
113 western basin with a maximum and minimum of 0.086 psu and 0.003, respectively.

114 Overall, for the period between 1993-2019 we note that the observational products, gridded using optimal interpolation
115 statistical techniques, show a higher average salinity compared to the reanalysis products that are dynamically integrated and
116 corrected through data assimilation. The spread is representing the offset of the products more than their variability in the
117 entire Mediterranean Sea, as well as in its eastern and western subdomains.

118 All the products show a positive trend between 1993-2019 (in parenthesis in Table 1). The trend in the mean of all products
119 is calculated as 0.0056 psu/year. This trend is consistent with the estimates between 1950-2002 of Skliris et al., (2018) from
120 EN4 and MEDATLAS data sets which shows a trend of 0.0096 ± 0.0077 and 0.0088 ± 0.0092 respectively, in the first 150
121 m while 0.0067 ± 0.0040 and 0.0067 ± 0.0036 between 150-600 m. The differences in trend in different products that we
122 used are mainly due to the discrepancies at the beginning of the timeseries. The weak consistency among the reanalyses
123 visible during the first decade is likely due to the lack of observations not sufficient to constrain the different models which
124 use different physics and initialization (e.g., Masina and Storto, 2017). The reduction of the spread among the products
125 evolves in parallel to the increase of the observational coverage after the advent of the ARGO network. The observational
126 products will be impacted from the scarcity of the observations in the '90s, since they rely on statistical methods. The trend
127 calculated for each grid point from the MEDREA24, which is the analysed product covering the longest period, is presented
128 in Fig. 2d. The dominant signal in the entire basin is positive with a larger amplitude in the Balearic Sea, Ionian Sea, Adriatic
129 Sea, Western Levantine and with a less evident signal in the Gulf of Lions, Northern Aegean Sea and Eastern Levantine
130 Basin. A small negative trend zone appears in the Alboran Sea. The trend in the entire analysed period is about 0.0049
131 psu/year in the western basin. This is below the rate of the basin-wide trend which is larger due to the trend in the eastern
132 basin (0.0061 psu/yr). Differences among different products, especially the objectively-analysed observations and GREP, for
133 the trend is larger in the western basin. They are more confined around the mean in the eastern basin which may explain also
134 the lower spread in this area as discussed below in Fig. (3b).

135 For 2020, CORA and ARMOR3D products are available, and both continue to sustain the positive trend even though it is
136 less evident in the western basin. MEDREA24 (and its interim extension) shows an increasing mean salinity until the end of
137 2021. All products present larger values after 2016 and a maximum in 2018.

138 The spatial mean, computed between 1993-2014 from all products in the first 300 m (Fig. 3a), shows a gradual increase in
139 the upper ocean integrated salinity from west to east. Minimum salinity occurs close to river mouths, such as in the North
140 Adriatic Sea due to the freshwater input from the Po River, and on the pathways of the outflow of the Dardanelles and
141 Gibraltar straits. The Atlantic water, modified through its route, can be traced till the eastern basin from its low salinity. The
142 spread deduced from all the products (Fig. 3b) implies that they agree more, meaning lower spread, in the Levantine and
143 Ionian Seas and to a lesser degree between the Balearic and Sardinia / Corsica islands. The spread is larger especially in the
144 northern Aegean and Adriatic Sea and southwestern coast between the Gulf of Gabes and Gibraltar Strait. This uncertainty
145 or mismatch in the products is possibly due to the different volume fluxes through the rivers and straits.

146 In Fig. 4 (a-c), we show the time series of the salinity anomaly estimates in the western (Fig. 4a), eastern (Fig. 4b) and entire
147 (Fig. 4c) basin from each product using formula (2). We recall that the salinity reference is computed for each product per
148 se. Moreover, the salinity anomaly map in 2021 from MEDREA24 is depicted in Fig. (4d), computed against the overall
149 mean between 1993-2014, which is shown in Fig. (3a).

150 The anomalies have a larger range in the reanalysis products. There is a negative anomaly within the first decade in GREP
151 and MEDREA24 which turns to positive first in the western Mediterranean (Fig. 4a) and followed by the eastern basin (Fig.
152 4b) after 2006. In the CORA and ARMOR3D, instead, there is a clear increase in the salinity anomaly in the eastern
153 Mediterranean and the entire basin with a less evident positive trend in the western basin. We summarise the mean salinity
154 anomalies in Table 2.

155 In 2021, the anomaly is mostly positive with some negative anomaly structures on the path of Atlantic water (Fig. 4d),
156 Alboran Sea, upwelling favouring Balearic Islands. Fedele et al. (2022) reports a positive salinity trend in the modified
157 Atlantic and Levantine intermediate waters using 18-year-long (2001-2019) Argo profiles, which in general agrees with the
158 anomaly map to a large extent. However, we note that the spread on the pathway of the water entering from the Gibraltar
159 strait and reaching the Levantine basin has a relatively larger spread compared to the deeper areas (see Fig. 3b).

160 **4 Conclusions**

161 In this study, we presented the salinity characteristics of the Mediterranean Sea in the upper 300 m deduced from various
162 products including reanalysis and gridded observational datasets released by Copernicus Marine Service. The products with
163 dynamically constructed ocean reanalysis and objectively analysed observations show significantly large spread at the
164 beginning of the period of investigation while the uncertainty reduces possibly with the emergence of ARGO profilers which
165 allowed a wider spatial and higher frequency sampling in the ocean. The mean salinity with its anomaly and trend is computed
166 and analysed in the entire basin as well as in the western and eastern basins for all the datasets separately and averaged. The
167 spatial maps of the mean and the spread of the salinity are depicted and discussed. The overall results show a salinification
168 of the Mediterranean Sea agreeing with earlier studies (e.g., Skliris et al. 2018). The subbasin scale investigation shows
169 negative salinity anomalies in the western basin in the upwelling regions, which may imply stronger upwelling events, and
170 waterway following the north African coast, which may be a consequence of the freshening North Atlantic water masses
171 (Holliday et al., 2020). There is a large spread in the salinity estimates among different products, which reduces with the
172 introduction of the Argo profilers in the data assimilation components of the reanalysis systems. Besides the large spread,
173 considering the reported discrepancies in the salinity measurements after 2016 (Barnoud et al., 2021), it is essential to use all
174 available information sources for a more accurate state estimate and uncertainty quantification.

175 **Data availability**

176 All datasets used in this article can be obtained from the Copernicus Marine Service catalogues as described in Table 3 with
177 their names, temporal coverages, and documentation.

178 **Acknowledgments**

179 This study has been conducted using EU Copernicus Marine Service Information. This work has been funded through the
180 EU Copernicus Marine Med-MFC Service Lot n. 21002L5-COP-MFC MED-5500.

181 **References**

182 Aagaard, K., and Carmack, E. C.: The role of sea ice and other fresh water in the Arctic circulation. *Journal of Geophysical*
183 *Research: Oceans*, 94(C10), 14485-14498. 1989.

184 Aydoğdu, A., Pinardi, N., Özsoy, E., Danabasoglu, G., Gürses, Ö., and Karspeck, A.: Circulation of the Turkish Straits
185 System under interannual atmospheric forcing. *Ocean Science*, 14(5), 999-1019. 2018.

186 Barnoud, A., Pfeffer, J., Guérou, A., Frery, M.-L., Siméon, M., Cazenave, A., et al.: Contributions of altimetry and Argo to
187 non-closure of the global mean sea level budget since 2016. *Geophysical Research Letters*, 48, e2021GL092824.
188 <https://doi.org/10.1029/2021GL092824>, 2021.

189 Blockley, E. W., Martin, M. J., McLaren, A. J., Ryan, A. G., Waters, J., Lea, D. J., ... and Storkey, D.: Recent development
190 of the Met Office operational ocean forecasting system: an overview and assessment of the new Global FOAM forecasts.
191 *Geoscientific Model Development*, 7(6), 2613-2638. 2014.

192 Boyer, T., Levitus, S., Antonov, J., Locarnini, R., Mishonov, A., Garcia, H., and Josey, S. A.: Changes in freshwater content
193 in the North Atlantic Ocean 1955–2006. *Geophysical Research Letters*, 34(16). 2007.

194 Bretherton, F. P., R. E. Davis and C. B. Fandry, A technique for objective analysis and design of oceanographic experiments
195 applied to MODE-73, 1976 / *Deep-Sea Res.*, 23, 559-582

196 Cessi, P., Pinardi, N., and Lyubartsev, V.: Energetics of semienclosed basins with two-layer flows at the strait. *Journal of*
197 *physical oceanography*, 44(3), 967-979. 2014.

198 Cheng, L., Trenberth, K. E., Gruber, N., Abraham, J. P., Fasullo, J. T., Li, G., Mann, M. E., Zhao, X., and Zhu, J.: Improved
199 Estimates of Changes in Upper Ocean Salinity and the Hydrological Cycle, *Journal of Climate*, 33(23), 10357-10381. doi:
200 [10.1175/J9-2022.2022.CLI-D-20-0366.1](https://doi.org/10.1175/J9-2022.2022.CLI-D-20-0366.1), 2020.

201 Cos, J., Doblas-Reyes, F., Jury, M., Marcos, R., Bretonnière, P.A., and Samsó, M.: The Mediterranean climate change hotspot
202 in the CMIP5 and CMIP6 projections, *Earth Syst. Dynam.*, 13, 321–340, <https://doi.org/10.5194/esd-13-321-2022>, 2022.

203 Dayan, H., McAdam, R., Masina, S., and Speich, S.: Diversity of marine heatwave trends across the Mediterranean Sea over
204 the last decades, in: Copernicus marine service ocean state report, issue 6, *Journal of Operational Oceanography*, vol. 15, pp.
205 49–56, 2022.

206 Escudier, R., Clementi, E., Omar, M., Cipollone, A., Pistoia, J., Aydogdu, A., Drudi, M., Grandi, A., Lyubartsev, V., Lecci,
207 R., Cretí, S., Masina, S., Coppini, G., & Pinardi, N. (2020). Mediterranean Sea Physical Reanalysis (CMEMS MED-Currents)
208 (Version 1) Data set. Copernicus Monitoring Environment Marine Service (CMEMS). <https://doi.org/10.25423>

209 Escudier, R., Clementi, E., Cipollone, A., Pistoia, J., Drudi, M., Grandi, A., Lyubartsev, V., Lecci, R., Aydogdu, A., Delrosso,
210 D., Omar, M., Masina, S., Coppini, G., and Pinardi, N. (2021) A High Resolution Reanalysis for the Mediterranean Sea.
211 *Front. Earth Sci.* 9:702285. doi: [10.3389/feart.2021.702285](https://doi.org/10.3389/feart.2021.702285), 2021.

212 Fedele, G., Mauri, E., Notarstefano, G., and Poulain, P. M.: Characterization of the Atlantic Water and Levantine Intermediate
213 Water in the Mediterranean Sea using 20 years of Argo data, *Ocean Sci.*, 18, 129–142, [https://doi.org/10.5194/os-18-129-](https://doi.org/10.5194/os-18-129-2022)
214 [2022](https://doi.org/10.5194/os-18-129-2022), 2022.

215 Guinehut, S., Dhomps, A-L., Larnicol, G., Le Traon, P-Y.: High resolution 3D temperature and salinity fields derived from
216 in situ and satellite observations. *Ocean Sci* 8:845–857. doi:[10.5194/os-8-845-2012](https://doi.org/10.5194/os-8-845-2012), 2012.

217 Holliday, N.P., Bersch, M., Berx, B., Chafik, L., Cunningham, S., Florindo-López, C., Hátún, H., Johns, W, Josey, SA.,
218 Larsen, K.M., Mulet, S.: Ocean circulation causes the largest freshening event for 120 years in eastern subpolar North
219 Atlantic. *Nat Commun* **11**, 585. <https://doi.org/10.1038/s41467-020-14474-y>, 2020.

220 Jarosz, E., Teague, W. J., Book, J. W., & Beşiktepe, Ş. T. (2013). Observed volume fluxes and mixing in the Dardanelles
221 Strait. *Journal of Geophysical Research: Oceans*, 118(10), 5007-5021.

222 Johnson G. C., Hosoda S., Jayne S. R., Oke P. R., Riser S. C., Roemmich D., Suga T., Thierry V., Wijffels S. E. and Xu, J.:
223 Argo-two decades: global oceanography, revolutionized. *Annual review of marine science*, 14, 379-403. 2022.

224 Jordà, G., Von Schuckmann, K., Josey, S. A., Caniaux, G., García-Lafuente, J., Sammartino, S., Özsoy E, Polcher J,
225 Notarstefano G, Poulain PM, Adloff F., Salat J., Naranjo C., Schroeder K., Chiggiato J., Sannino G., and Macías, D.: The
226 Mediterranean Sea heat and mass budgets: Estimates, uncertainties and perspectives. *Progress in Oceanography*, 156, 174-
227 208. <https://doi.org/10.1016/j.pocean.2017.07.001>, 2017.

228 Juza, M, Fernández-Mora, À, and Tintoré, J.: Sub-Regional Marine Heat Waves in the Mediterranean Sea From Observations:
229 Long-Term Surface Changes, Sub-Surface and Coastal Responses. *Front. Mar. Sci.* 9:785771. doi:
230 [10.3389/fmars.2022.785771](https://doi.org/10.3389/fmars.2022.785771), 2022.

231 Lellouche, J. M., Le Galloudec, O., Drévilion, M., Régnier, C., Greiner, E., Garric, G., ... and De Nicola, C.: Evaluation of
232 global monitoring and forecasting systems at Mercator Océan. *Ocean Science*, 9(1), 57-81. 2013.

233 Masina S., and Storto, A., 2017. Reconstructing the recent past ocean variability: status and perspective. *Journal of Marine*
234 *Research*, 75, (6), pp. 727-764(38).

235 Pisano, A., Marullo, S., Artale, V., Falcini, F., Yang, C., Leonelli FE, Santoleri, R., and Buongiorno Nardelli, B.: New
236 Evidence of Mediterranean Climate Change and Variability from Sea Surface Temperature Observations. *Remote Sensing*,
237 12(1):132. <https://doi.org/10.3390/rs12010132>, 2020.

238 Sannino, G., Sözer, A., and Özsoy, E.: A high-resolution modelling study of the Turkish Straits System. *Ocean Dynamics*,
239 67(3), 397-432. 2017.

240 Schauer, U., and Losch, M.: “Freshwater” in the ocean is not a useful parameter in climate research. *Journal of Physical*
241 *Oceanography*, 49(9), 2309-2321. 2019.

242 Schroeder, K., Chiggiato, J., Bryden, H. L., Borghini, M., and Ben Ismail, S.: Abrupt climate shift in the Western
243 Mediterranean Sea. *Scientific reports*, 6(1), 1-7. 2016.

244 Skliris, N., Zika, J. D., Herold, L., Josey, S. A., and Marsh, R.: Mediterranean sea water budget long-term trend inferred from
245 salinity observations. *Climate Dynamics*, 51(7), 2857-2876. <https://doi.org/10.1007/s00382-017-4053-7>, 2018.

246 Soto-Navarro, J., Criado-Aldeanueva, F., García-Lafuente, J., & Sánchez-Román, A. (2010). Estimation of the Atlantic
247 inflow through the Strait of Gibraltar from climatological and in situ data. *Journal of Geophysical Research: Oceans*,
248 115(C10).

249 Storto, A., Masina, S. and Navarra, A.: Evaluation of the CMCC eddy-permitting global ocean physical reanalysis system
250 (C-GLORS, 1982–2012) and its assimilation components. *Q.J.R. Meteorol. Soc.*, 142: 738–758. doi:10.1002/qj.2673, 2016.

251 Storto, A., Masina, S., Simoncelli, S. et al.: The added value of the multi-system spread information for ocean heat content
252 and steric sea level investigations in the CMEMS GREP ensemble reanalysis product. *Clim Dyn* 53, 287–312.
253 <https://doi.org/10.1007/s00382-018-4585-5>, 2019a.

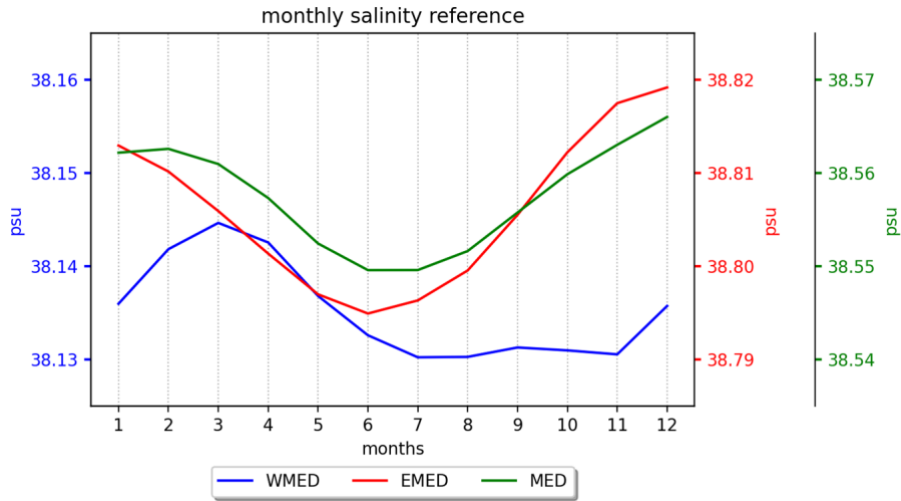
254 Storto, A., Alvera-Azcárate, A., Balmaseda, M. A., Barth, A., Chevallier, M., Counillon, F., ... and Zuo, H.: Ocean reanalyses:
255 recent advances and unsolved challenges. *Frontiers in Marine Science*, 6, 418. 2019b.

256 Szekely, T., Gourrion, J., Pouliquen, S., and Reverdin, G.: The CORA 5.2 dataset for global in situ temperature and salinity
257 measurements: data description and validation, *Ocean Sci.*, 15, 1601–1614, <https://doi.org/10.5194/os-15-1601-2019>, 2019.

258 Tuel, A., and Eltahir, E. A. B.: Why Is the Mediterranean a Climate Change Hot Spot?, *Journal of Climate*, 33(14), 5829-
259 5843. Retrieved Jan 25, 2022, from <https://journals.ametsoc.org/view/journals/clim/33/14/JCLI-D-19-0910.1.xml>, 2020.

260 Zunino, P., Schroeder, K., Vargas-Yáñez, M., Gasparini, G. P., Coppola, L., García-Martínez, M. C. and Moya-Ruiz, F.:
261 Effects of the Western Mediterranean Transition on the resident water masses: Pure warming, pure freshening and pure
262 heaving. *Journal of Marine Systems* 15, 96–97. doi: [10.1016/j.jmarsys.2012.01.011](https://doi.org/10.1016/j.jmarsys.2012.01.011), 2012.

263 Zuo, H., Balmaseda, M. A., and Mogensen, K.: The new eddy-permitting ORAP5 ocean reanalysis: description, evaluation
264 and uncertainties in climate signals. *Clim. Dyn.* 49, 791–811. doi: [10.1007/s00382-015-2675-1](https://doi.org/10.1007/s00382-015-2675-1), 2017.



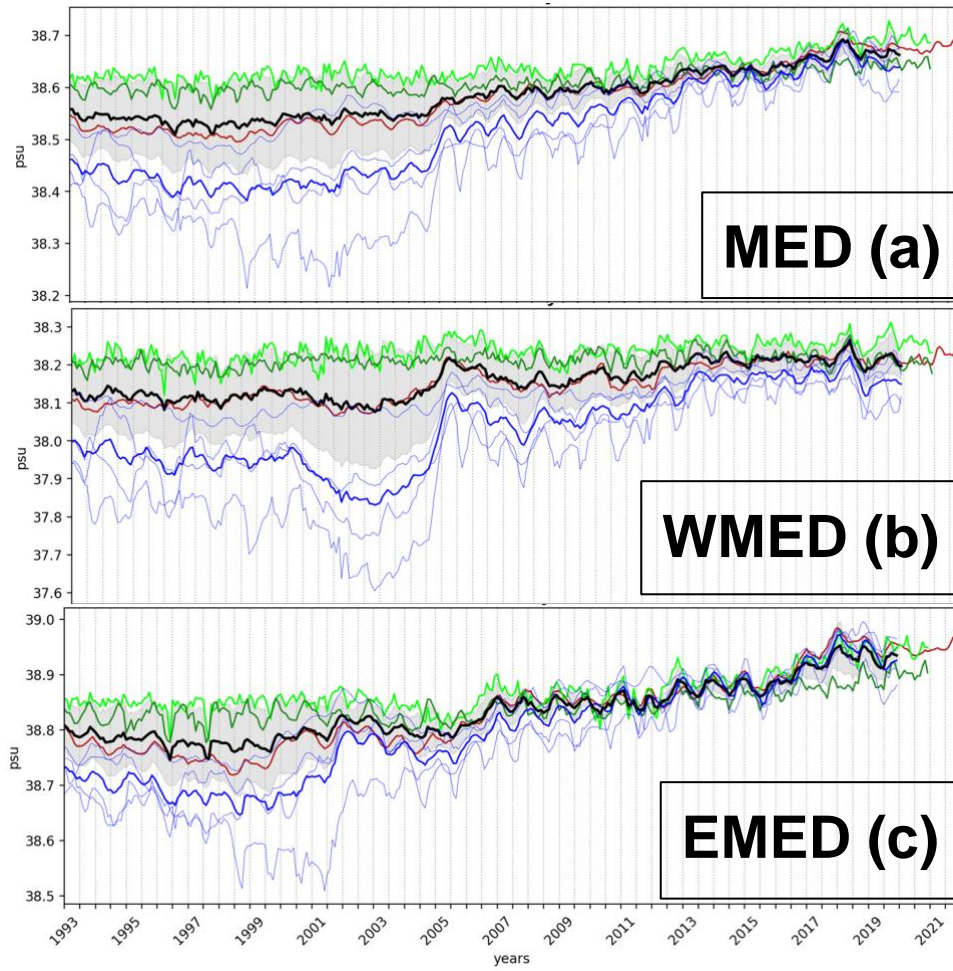
265

266 **Figure 1:** The monthly reference salinity S_{ref} estimates calculated from the MEDREA24 in the period 1993-2014. The green,
 267 blue, and red curves show the MED, WMED and EMED regions respectively on its corresponding vertical axis. The same
 268 calculation is done for each product separately (not shown) to evaluate formula (2) to compute salinity anomaly.

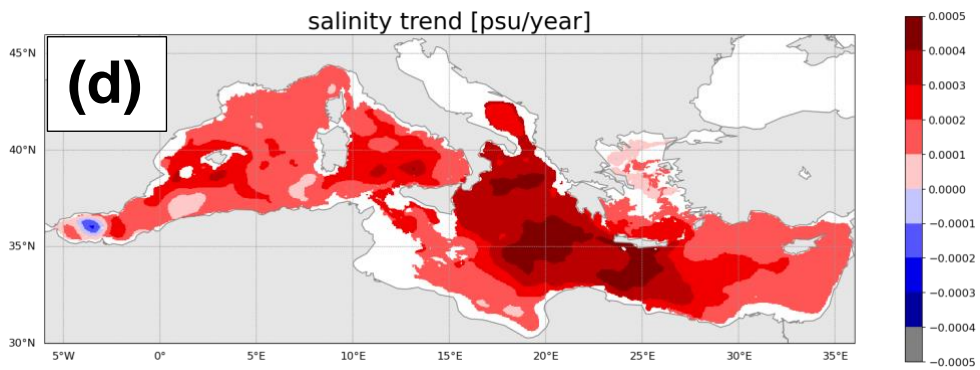
269

| psu (psu/year) | MED | WMED | EMED |
|-----------------|----------------|----------------|----------------|
| MEDREA24 | 38.58 (0.0070) | 38.15 (0.0055) | 38.83 (0.0078) |
| GREP | 38.48 (0.0110) | 38.01 (0.0111) | 38.87(0.0106) |
| CORA | 38.61 (0.0020) | 38.21(0.0019) | 38.84 (0.0024) |
| ARMOR3D | 38.64 (0.0027) | 38.24 (0.0020) | 38.75(0.0032) |
| mean | 38.57 (0.0056) | 38.16 (0.0049) | 38.87 (0.0061) |

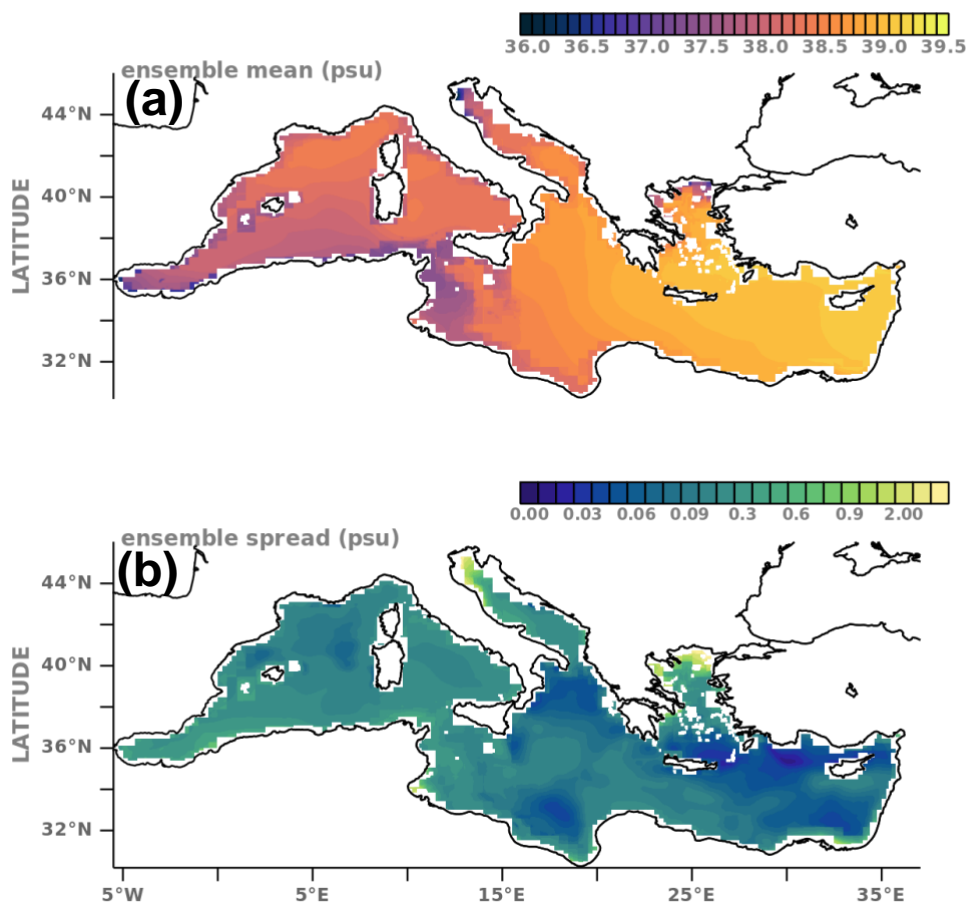
270 **Table 1.** The temporal mean salinity (in psu) and trend (in psu per year) in the 0-300 m between the common period 1993-
 271 2019 for separate products and their overall mean in Fig. 2.



— MEDREA24 — ARMOR3D — CORA — GREP — mean \pm std



273 **Figure 2:** Time series of mean salinity in the upper 300 m in the (a) entire Mediterranean Sea (b) western Mediterranean
 274 basin and (c) eastern Mediterranean basin between the period 1993 and 2021 from MEDREA24, until the end of 2020 for
 275 ARMOR3D, CORA and until the end of 2019 for GREP. The mean of all the products is drawn in black with their standard
 276 deviation shaded around the mean. GREP ensemble members are depicted in thin blue curves. The GREP product covers the
 277 period until 2019 while the observational products CORA and ARMOR3D cover until 2020. The time series for MEDREA24
 278 is extended until 2021 using the interim products. (d) salinity trend in the first 300 m. from the MEDREA24 psu per year.

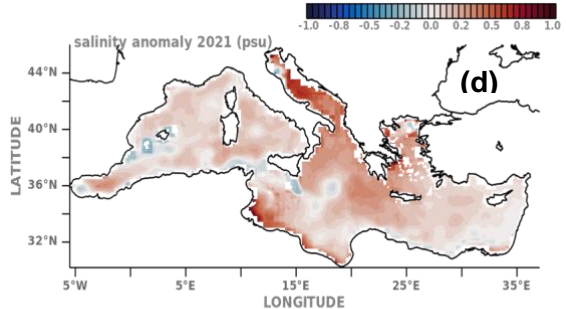
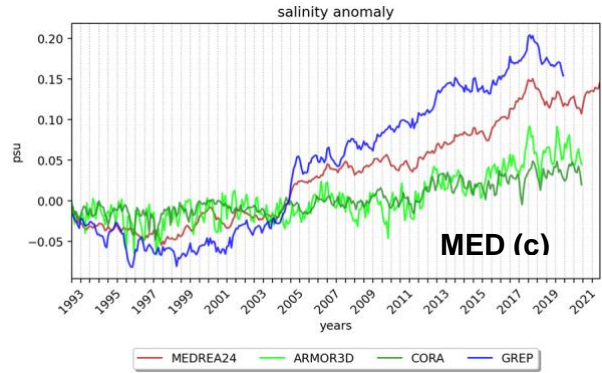
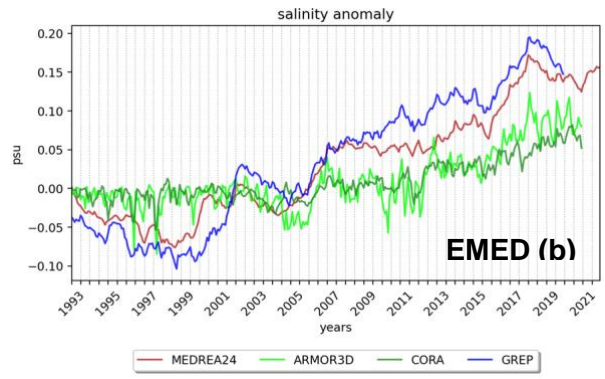
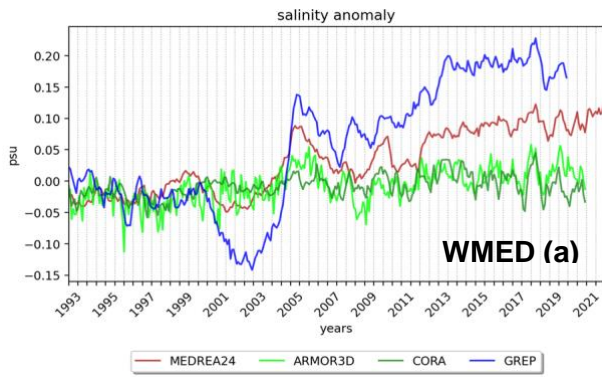


279

280 **Figure 3.** The maps of (a) mean and (b) spread of integrated salinity in the period between 1993–2014 in 0-300 m. computed
 281 from the GREP ensemble mean, CORA, ARMOR3D and MEDREA24 products. We refer to the text for the information on
 282 the data products used. The analysis is performed only if the water column is deeper than 300 m. Note that in (b) the colour
 283 scale is not linear to show the smaller standard deviation.

| psu | MED | WMED | EMED |
|-----------------|------------|-------------|-------------|
| MEDREA24 | 0.026 | 0.027 | 0.025 |
| GREP | 0.042 | 0.056 | 0.034 |
| CORA | 0.001 | -0.008 | 0.007 |
| ARMOR3D | 0.001 | -0.009 | 0.008 |
| mean | 0.018 | 0.017 | 0.019 |

285 **Table 2.** The temporal mean salinity anomaly (in psu) in the 0-300 m between the common period 1993-2019 for separate
 286 products and their average in *Fig. 3*.



288

289 **Figure 4.** Time series of salinity anomaly from the MEDREA24, GREP, ARMOR3D and CORA products in the (a) western
 290 Mediterranean Sea (b) eastern Mediterranean basin and (c) entire Mediterranean basin computed with respect to the monthly
 291 reference salinity estimates in the corresponding area in Fig. 1 calculated from the MEDREA24 in the period 1993-2014.
 292 The GREP products cover the period until 2019 while the observational products CORA and ARMOR3D covers until 2020.
 293 The time series for MEDREA24 is extended until 2021 using the interim products. (d) salinity anomaly in 2021 in the
 294 Mediterranean Sea against the mean of salinity in Fig. 3a.

| | Product Name | Documentation | Data access / Time Period |
|--------------------------------------|---|--|---|
| Mediterranean Sea Physics Reanalysis | MEDSEA_MU LTIYEAR_PH Y_006_004; Numerical models | Product User Manual (CMEMS-MED-PUM-006-004) Quality Information Document (CMEMS-MED-QUID-006-004) https://resources.marine.copernicus.eu/product-detail/MEDSEA_MULTIYEAR_PHY_006_004/DOCUMENTATION Escudier et al., (2020) | EU Copernicus Marine Service Product 2022 / 1987-2021 |

| | | | |
|--|--|--|---|
| Global Ocean Ensemble Physics Reanalysis | GLOBAL_REANALYSIS_PHY_001_031; Numerical models | Product User Manual (CMEMS-GLO-PUM-001-031) Quality Information Document (CMEMS-GLO-QUID-001-031) https://resources.marine.copernicus.eu/product-detail/GLOBAL_REANALYSIS_PHY_001_031/DOCUMENTATION | EU Copernicus Marine Service Product 2022 / 1993-2019 |
| Global Ocean-Delayed Mode gridded CORA-In-situ Observations objective analysis in Delayed Mode | INSITU_GLO_TS_OA_REP_OBSERVATIONS_013_002_b; Observations | Product User Manual (CMEMS-INS-PUM-013-002-ab) Quality Information Document (CMEMS-INS-QUID-013-002b) https://resources.marine.copernicus.eu/product-detail/INSITU_GLO_TS_OA_REP_OBSERVATIONS_013_002_b/DOCUMENTATION | EU Copernicus Marine Service Product 2022 / 1993-2020 |
| Multi Observation Global Ocean 3D Temperature Salinity Height Geostrophic Current and MLD | MULTIOBS_GLO_PHY_TSUV_3D_MYNRT_015_012; Observations | Product User Manual (CMEMS-MOB-PUM-015-012) Quality Information Document (CMEMS-MOB-QUID-015-012) https://resources.marine.copernicus.eu/product-detail/MULTIOBS_GLO_PHY_TSUV_3D_MYNRT_015_012/DOCUMENTATION Guinehut et al., (2012) | EU Copernicus Marine Service Product 2022 / 1993-2020 |

295 **Table 3.** Products from Copernicus Marine Service used in this study.